ANALYTICAL SCIENCES NOVEMBER 2011, VOL. 27

Reviews

UV Raman Markers for Structural Analysis of Aromatic Side Chains in Proteins

Hideo TAKEUCHI

Graduate School of Pharmaceutical Sciences, Tohoku University, Aobayama, Sendai 980–8578, Japan

UV Raman spectroscopy is a powerful tool for investigating the structures and interactions of the aromatic side chains of Phe, Tyr, Trp, and His in proteins. This is because Raman bands of aromatic ring vibrations are selectively enhanced with UV excitation, and intensities and wavenumbers of Raman bands sensitively reflect structures and interactions. Interpretation of protein Raman spectra is greatly assisted by using empirical correlations between spectra and structure. Many Raman bands of aromatic side chains have been proposed to be useful as markers of structures and interactions on the basis of empirical correlations. This article reviews the usefulness and limitations of the Raman markers for protonation/deprotonation, conformation, metal coordination, environmental polarity, hydrogen bonding, hydrophobic interaction, and cation-π interaction of the aromatic side chains. The utility of Raman markers is demonstrated through an application to the structural analysis of a membrane-bound proton channel protein.

(Received August 10, 2011; Accepted August 29, 2011; Published November 10, 2011)

1 Introduction

A protein is comprised of one or more linear polymers of amino acids connected by peptide bonds (Fig. 1). The formation of a peptide bond by dehydration reaction produces planar amide groups between two successive amino acids, and the C_α atom of each amino acid bridges two amide groups forming the peptide main chain. The side chains of amino acids stick out from the main chain at the C_α position. Usually, up to twenty kinds of amino acids differing in side chain structure are used to construct proteins in living organisms. The sequence of amino acids in a polypeptide chain is the determinant of the three-dimensional structure of the protein, and the function of the protein is closely related to the structure. Structural analysis of proteins is thus important to understand the molecular mechanisms of protein functions.

Among the twenty standard amino acids, phenylalanine (Phe), tyrosine (Tyr), tryptophan (Trp), and histidine (His) are classified into the group of aromatic amino acids because they contain an aromatic ring (benzene, phenol, indole, or imidazole ring, respectively) in the side chain (Fig. 1). The aromatic rings of these amino acids are electron-rich and bulky compared to the side chains of most other amino acids, and they can be involved in hydrophobic (Phe, Tyr, and Trp), hydrogen bonding (Tyr, Trp, and His), cation-π (Phe, Tyr, Trp, and His), and other interactions with nearby residues or with exogenous components. The planarity of the aromatic ring limits the conformational freedom of the side chain, and the orientation of the ring plane sometimes plays an important role in the interaction. These unique properties of aromatic amino acids are fully utilized in the structural formation and the functional performance of proteins.

Raman spectroscopy is a tool for observing molecular vibrations by using inelastic light (photon) scattering.[1] The energy of a photon impinging on a molecule is partially absorbed by a vibration of the molecule, and a photon with decreased energy is scattered from the molecule. (Raman scattering with

Hideo TAKEUCHI received his BS, MS, and PhD degrees in chemistry from the University of Tokyo in 1971, 1973, and 1976, respectively. After a one-year post-doctoral research at Imperial College London, he became a research associate of the University of Tokyo in 1977. He moved to the Graduate School of Pharmaceutical Sciences, Tohoku University in 1981 and has been serving as a professor of bio-structural chemistry since 1993. His current research interest is the spectroscopic analysis of structural and functional aspects of disease-related proteins.

E-mail: takeuchi@m.tohoku.ac.jp

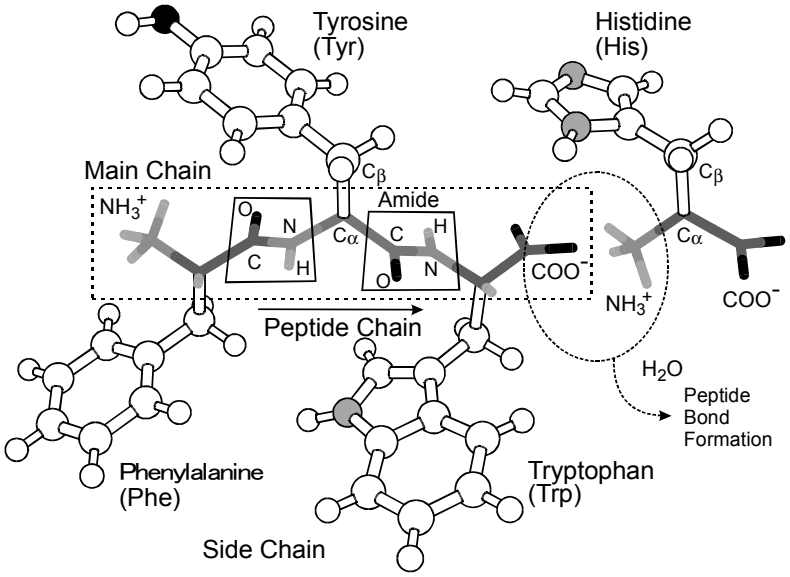

Fig. 1 Formation of a peptide chain and the structures of four aromatic residues Phe, Tyr, Trp, and His. Nitrogen and oxygen atoms in the side chains are presented in gray and black, respectively.

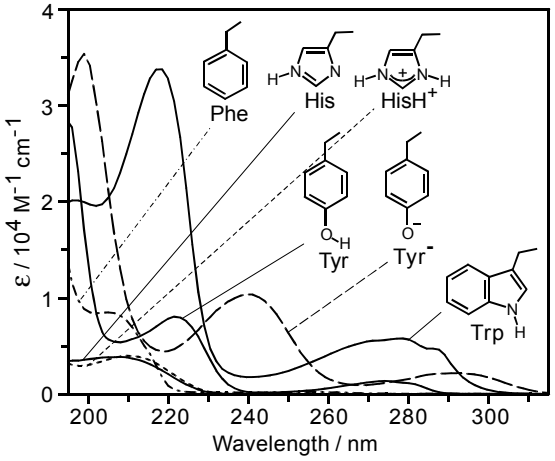

Fig. 2 UV absorption spectra of aromatic amino acids in H_2O solution.

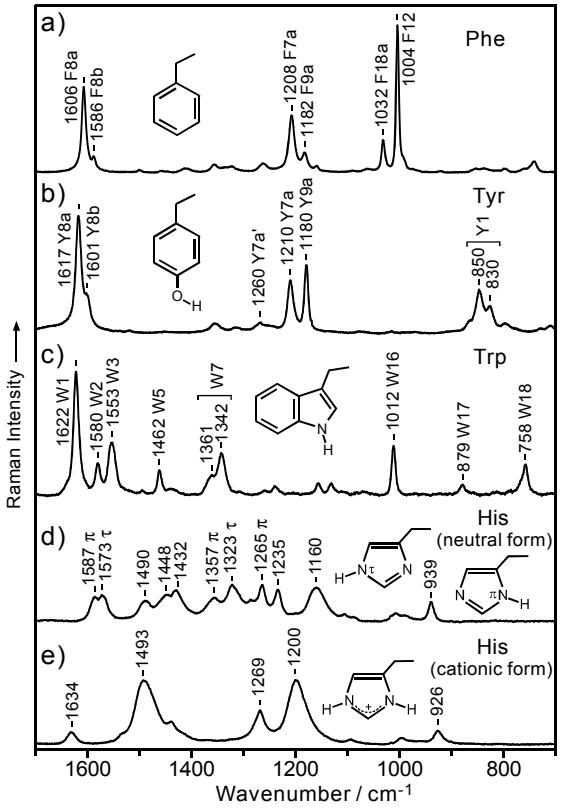

Fig. 3 UV Raman spectra of a) Phe, b) Tyr, c) Trp, d) neutral His, and e) cationic His. Strong Raman bands due to aromatic ring vibrations of Phe, Tyr, and Trp are marked with the one-letter code of the amino acid (F, Y, or W) followed by the vibrational mode number.[6] The spectra were recorded in H_2O solution with 229-nm excitation for Phe and His or with 244-nm excitation for Tyr and Trp.

energy gain is also possible but weaker than the commonly observed energy loss scattering.) The energy difference between the incident and scattered photons corresponds to the energy of vibration and is usually expressed in units of wavenumbers (cm^{-1}). In the Raman spectrum, the intensity of scattered light is plotted against the wavenumber. The wavelength of the light used to excite a molecule for Raman scattering observation is called the excitation wavelength. When the excitation wavelength is close to or within one of the electronic absorption bands of the molecule, strong Raman scattering occurs from some molecular vibrations that are coupled (resonant) with the electronic transition responsible for the absorption band. Such resonance enhancement of Raman intensity sometimes amounts to about four orders of magnitude.[2,3]

The aromatic rings of Phe, Tyr, Trp, and His exhibit absorption bands due to π-π* transitions in the UV region (Fig. 2), and excitation of the aromatic residues with UV light produces resonance enhancement of Raman scattering from the aromatic rings. Figure 3 shows the Raman spectra of Phe, Tyr, Trp, and His recorded with an excitation wavelength of 229 or 244 nm. The Raman bands in these spectra are all ascribed to aromatic ring vibrations resonant with one or more π-π* transitions,[4-9]

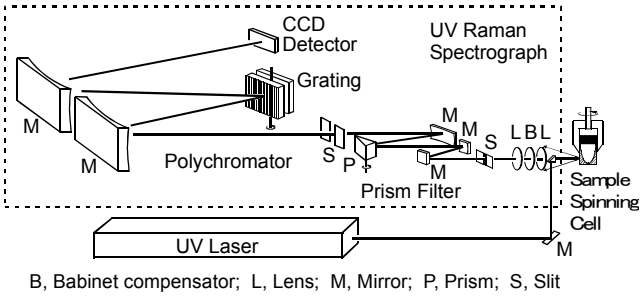

Fig. 4 Schematic drawing of a UV Raman spectrometric system.

while vibrations of non-aromatic parts of the molecule are not detected in the spectra. Some strong bands of Phe, Tyr, and Trp are marked with the one-letter code of the amino acid (F, Y, or W) followed by the vibrational mode number. Such selective enhancement of Raman intensity for aromatic ring vibrations also occurs in UV Raman spectra of proteins, eliminating interference from the other parts of the protein or from solvents and allowing structural studies at low concentrations relevant to physiological levels. This article reviews the utility and methodology of UV Raman spectroscopy in the structural analysis of protein aromatic side chains.

2 UV Raman Instrumentation

A typical UV Raman spectrometric system consists of a UV laser for excitation of Raman scattering, a spinning quartz cell for minimizing the sample damage caused by UV irradiation, and a spectrograph for dispersing and detecting the Raman scattered light (Fig. 4). Among UV lasers, the lasers operating in a continuous mode are preferred to those of pulsed mode because the high peak power of laser pulses tends to induce photochemical damage in the sample. To obtain high-quality UV Raman spectra with a low power of UV irradiation, one requires a high-throughput spectrograph and a highly sensitive detector. In our laboratory, a spectrograph equipped with a prism filter was developed to gain a high throughput of Raman scattered light and to efficiently eliminate interfering light, *i.e.* non-elastically scattered laser light (Rayleigh scattering) in the shorter wavelength region and fluorescence from the sample in the longer wavelength region.[10] High-performance UV detection with a minimized background dark signal is achieved by using a back-illuminated, UV/anti-reflection-coated, liquid-nitrogen-cooled CCD detector.

3 Raman Markers of Structures and Interactions

The wavenumber and intensity of a Raman band reflect the structure and interaction of the vibrating atomic group that is responsible for the Raman band. To fully exploit the Raman signals from a protein, it is necessary to assign the observed Raman bands to specific parts of the protein and then to interpret the wavenumbers and intensities of individual Raman bands in terms of structure and interaction. Interpretation of protein Raman spectra is greatly assisted by spectra-structure correlations, which are, in most cases, empirically derived from Raman spectra of small model compounds in crystals with known structure or dissolved in solvents with various properties. The Raman bands that can be used to extract structural information from Raman spectra are called "Raman makers." For aromatic side chains, many useful Raman markers have been reported and some of them will be reviewed below.

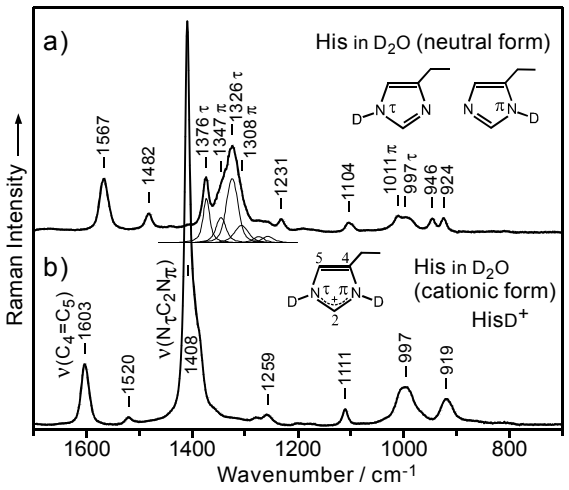

Fig. 5 UV Raman spectra of His in D_2O solution. a) His in the neutral form at neutral-to-alkaline pD, and b) His in the cationic form ($HisD^+$) at acidic pD. The spectra were excited at 229 nm.

3·1 Protonation/deprotonation

Protonation or deprotonation is possible in the aromatic side chains of Tyr and His. The pK_a values of these aromatic side chains in proteins are reported to be 10.3 ± 1.2 for Tyr and 6.6 ± 1.0 for His.[11] Although the deprotonation of the phenolic OH group of Tyr is unlikely to occur at physiological pH, deprotonated Tyr (Tyr^-), if present, can be readily detected by UV Raman spectroscopy because the L_a absorption band shifts from 220 to 240 nm upon deprotonation (Fig. 2), and excitation at ~240 nm produces selective resonance enhancement of the Raman bands of Tyr^-.[7,8] The deprotonation also causes shifts of the Y8a, Y8b, and Y9a bands at 1617, 1601, and 1180 cm^{-1} (Fig. 3b) by about –15, –40, and –5 cm^{-1}, respectively.[6,8]

The imidazole side chain of His carries two nitrogen atoms, N_τ and N_π (Fig. 3d). In the neutral form, one of the nitrogen atoms is protonated, while the other is deprotonated. The N_τ-H and N_π-H tautomers are in equilibrium with each other at neutral or alkaline pH, giving Raman bands assignable to one or both tautomers (Fig. 3d).[12-15] At acidic pH values below the pK_a (6.6), both nitrogen atoms are protonated to form cationic imidazolium ($HisH^+$). The Raman spectrum of His is strongly dependent on the state of protonation, as shown in Figs. 3d and 3e. Because the UV absorption of His is weak compared to the other aromatic residues (Fig. 2), the Raman bands of His are also weak. In D_2O solution, however, the *N*-deuterated cationic form ($HisD^+$) gives a strong band at 1408 cm^{-1} (Fig. 5), which is ascribed to the symmetric stretch of the N_τ–C_2–N_π linkage, $\nu(N_\tau C_2 N_\pi)$.[16] The intensity of the 1408 cm^{-1} band is comparable to those of Raman bands due to other aromatic residues and can be used to monitor the protonation of His residues in proteins.[15,17-21]

3·2 Conformation

The wavenumbers and modes of molecular vibrations are sensitive to the conformation of the molecule. Raman spectroscopy monitoring the molecular vibration is thus an

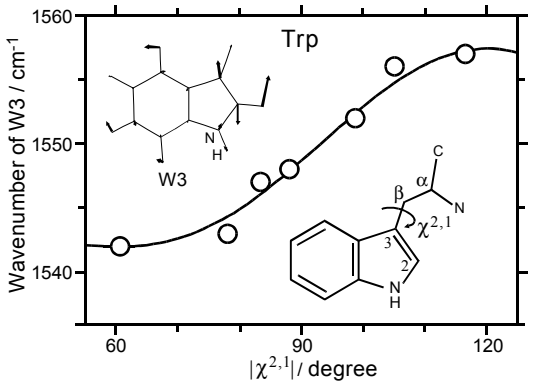

Fig. 6 Plot of the W3 wavenumber against the absolute value of $\chi^{2,1}$ observed for seven crystals of Trp and its derivatives with known structure.[23]

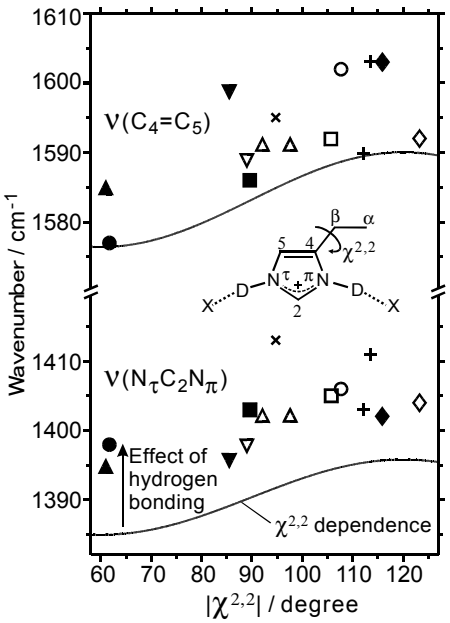

Fig. 7 Plots of the $\nu(C_4{=}C_5)$ and $\nu(N_\tau C_2 N_\pi)$ wavenumbers against the absolute value of $\chi^{2,2}$. The data were observed for twelve crystals of His and its derivatives,[30] which are marked with different symbols. The crystals marked with triangle and plus sign contain two inequivalent molecules in the unit cell. The solid curve shows the conformational dependence. The hydrogen bonding contribution to the wavenumber is indicated by the distance of the data point from the solid curve.

appropriate tool for studying molecular conformation. Although the aromatic rings of Phe, Tyr, Trp, and His are planar and have no conformational freedom within the aromatic ring, the peripheral linkage connecting the aromatic ring to the peptide main chain, C(ring)-C_β-C_α, has conformational freedom. Of the two C-C bonds, the torsion about the C(ring)-C_β bond has a possibility to influence the aromatic ring vibrations because of its direct attachment to the ring. So far, conformational dependence has been reported for a few ring vibrations of Trp and His. Phe and Tyr, having higher torsional symmetry about the C(ring)-C_β bond, may be less sensitive to the conformation than Trp and His.

The W3 Raman band of Trp at ~1550 cm^{-1} (Fig. 3c) arises from an indole ring vibration mainly contributed from the $C_2{=}C_3$ stretch.[22] From its vibrational mode, the wavenumber of W3 is expected to be affected by the torsion angle ($\chi^{2,1}$) of the $C_2{=}C_3$-C_β-C_α linkage. Figure 6 shows a plot of the W3 wavenumber (ν) against the absolute value of the torsion angle ($|\chi^{2,1}|$) observed for seven crystals of Trp and its derivatives with known structure.[23] The plot can be fitted by the following equation:[24]

$$\nu = 1541.8 + [6.9\cos(3|\chi^{2,1}|) + 1]^{1.2} \quad (1)$$

The $|\chi^{2,1}|$ dependence in Eq. (1) appears complicated, but the equation is almost identical to simpler Eq. (2).

$$\nu = 1549.2 + 8.1\cos(3|\chi^{2,1}|) \quad (2)$$

The threefold cosine dependence on $|\chi^{2,1}|$ may be due to an interaction between the π orbitals of the indole ring and the sp^3 hybrid orbitals of C_β through the torsional axis C_3-C_β. A very similar $|\chi^{2,1}|$ dependence was observed for an analog of Trp with deuterated ring carbons, Trp-2,4,5,6,7-d_5,[24] confirming that the W3 wavenumber serves as a marker of $|\chi^{2,1}|$. The orientation of the indole ring with respect to the peptide main chain is affected not only by $\chi^{2,1}$ but also by another torsional angle (χ^1) of the C_3-C_β-C_α-N linkage. In proteins, the χ^1 value is restricted to a few regions of rotational space depending on the secondary structure of the polypeptide chain.[25] If the χ^1 angle is limited to a few values by the secondary structure, the $|\chi^{2,1}|$ value determined by Raman spectroscopy can be used in building plausible orientation models of the Trp indole ring in the protein structure.[26-28]

Conformational dependence has also been found for two Raman bands of *N*-deuterated imidazolium, $HisD^+$.[29,30] As Fig. 5b shows, $HisD^+$ gives two strong Raman bands, $\nu(C_4{=}C_5)$ around 1600 cm^{-1} and $\nu(N_\tau C_2 N_\pi)$ around 1410 cm^{-1}. Their wavenumbers observed in twelve crystals of His and its derivatives with known structure are plotted against the absolute value of the $\chi^{2,2}$ torsional angle of the $C_5{=}C_4$-C_β-C_α linkage in Fig. 7.[30] The deviation of the data points from a smooth curve is ascribed to the fact that the wavenumbers of these two Raman bands are affected by hydrogen bonding as well. Including the hydrogen bonding effect, the observed wavenumber ν is well approximated by the following equation:[30]

$$\nu = \nu_0 + C\cos(3|\chi^{2,2}|) + H_\tau r_\tau^{-6} + H_\pi r_\pi^{-6} \quad (3)$$

where r_τ and r_π are the distances of X···H at the N_τ and N_π sites. Since r_τ and r_π are shorter in stronger hydrogen bonds, r_τ^{-6} and r_π^{-6} are a measure of the strength of hydrogen bonding. The constants ν_0, C, H_τ, and H_π are 1583.2 cm^{-1}, 6.8 cm^{-1}, 32.6×10^{-5} cm^{-1} nm^6, and -11.8×10^{-5} cm^{-1} nm^6, respectively, for $\nu(C_4{=}C_5)$, while they are 1390.4 cm^{-1}, 5.4 cm^{-1}, 3.7×10^{-5} cm^{-1} nm^6, and 20.7×10^{-5} cm^{-1} nm^6 for $\nu(N_\tau C_2 N_\pi)$. As in the case of Trp, a threefold cosine dependence is evident from Fig. 7, indicating that both $\nu(C_4{=}C_5)$ and $\nu(N_\tau C_2 N_\pi)$ are basically dependent on the torsional angle $|\chi^{2,2}|$. Additionally, the hydrogen bonding at N_τ increases the $\nu(C_4{=}C_5)$ wavenumber, whereas that at N_π decreases the $\nu(C_4{=}C_5)$ wavenumber and increases the $\nu(N_\tau C_2 N_\pi)$ wavenumber.

3·3 Metal coordination

The nitrogen atoms of the His imidazole ring serve as binding sites for divalent metal ions such as Cu^{2+} and Zn^{2+}. This property of the His side chain is exploited in binding and activating metal ions that are needed to perform protein functions. At neutral or

alkaline pH, His exists as one of the N_τ–H and N_π–H tautomers described in Sect. 3·1, and each tautomer has one free nitrogen atom, to which a metal ion can bind. Under special conditions, N_τ and N_π bind different metal ions and an imidazolate bridge is formed between the two metal ions. Metal binding affects the electron distribution over the imidazole ring, resulting in wavenumber changes of some ring vibrations.

Examination of Raman spectra of metal-bound His and its analogs in the crystalline state and in solution has revealed that $\nu(C_4{=}C_5)$ and a few ring stretch vibrations can be used as markers of metal binding.[31] As Fig. 8 shows, the $\nu(C_4{=}C_5)$ wavenumber of the N_π–H tautomer increases from 1587 cm^{-1} (Fig. 3d) to 1606 – 1594 cm^{-1} when a metal ion binds to N_τ. Additionally, a Raman band due to a ring stretch mode of the metal-bound form appears at 1440 – 1434 cm^{-1}. For the N_τ–H tautomer, the $\nu(C_4{=}C_5)$ wavenumber increases from 1573 cm^{-1} (Fig. 3d) to 1590 – 1573 cm^{-1} and a ring stretch band appears at 1277 – 1272 cm^{-1} upon metal binding to N_π. The imidazolate bridge is characterized by a $\nu(C_4{=}C_5)$ band at 1567 – 1555 cm^{-1} and a ring stretch band at 1292 – 1282 cm^{-1}. Generally, metal coordination shortens the $C_4{=}C_5$ bond and raises the $\nu(C_4{=}C_5)$ wavenumber of neutral His,[32] suggesting the utility of $\nu(C_4{=}C_5)$ as a measure of the strength of metal coordination.

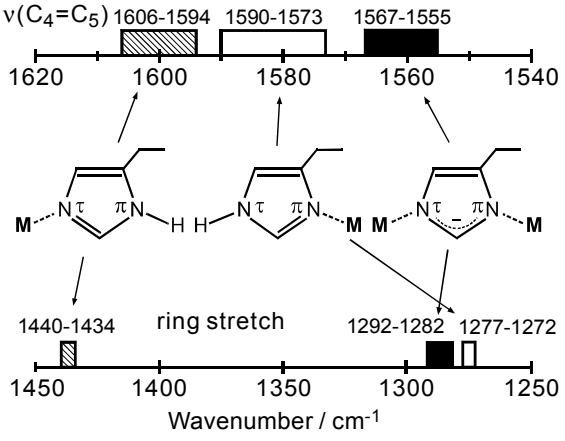

Fig. 8 Wavenumbers of $\nu(C_4{=}C_5)$ (upper bar) and ring vibrations (lower bar) characteristic of three metal-bound forms of His.[31]

3·4 Environmental polarity

The polarity of the environment does not directly affect the wavenumbers of Raman bands because Raman-active vibrations are not usually accompanied by a significant change of electric dipole moment that interacts with the environmental polarity. However, intensities of Raman bands are influenced by the environmental polarity through electronic transitions, in particular under resonance conditions. This is because electronic states are affected by the environmental polarity and resonance enhancement of Raman scattering strongly depends on the intensity of electronic absorption near the Raman excitation wavelength.

Figure 9 shows UV absorption spectra of *N*-acetyl-L-phenylalanine ethyl ester (AcPheEE), *N*-acetyl-L-tyrosine ethyl ester (AcTyrEE), and 3-methylindole (skatole) dissolved in various solvents.[33,34] Since the benzene ring of Phe does not form hydrogen bonds, the solvent effect on the UV absorption spectrum of AcPheEE is ascribed to environmental polarity and/or polarizability. In Fig. 9a, the L_a absorption of Phe in the 200 – 260 nm region is stronger in CH_3OH than in H_2O and CH_3CN. Since the polarity of CH_3OH is much lower than those of H_2O and CH_3CN,[35,36] the change of absorption spectrum suggests that the Phe side chain gives stronger Raman scattering in less polar environments if the excitation wavelength is within the above-mentioned UV region. Actually, the F12 Raman band of Phe at 1004 cm^{-1} (Fig. 3a), which is resonant with the L_a transition,[7,9,37] has been reported to be enhanced up to twice by a decrease of environmental polarity when excited at 220 – 240 nm.[33,38,39] It has also been found that the Raman intensity change is much larger than the change of absorption intensity at the excitation wavelength. These

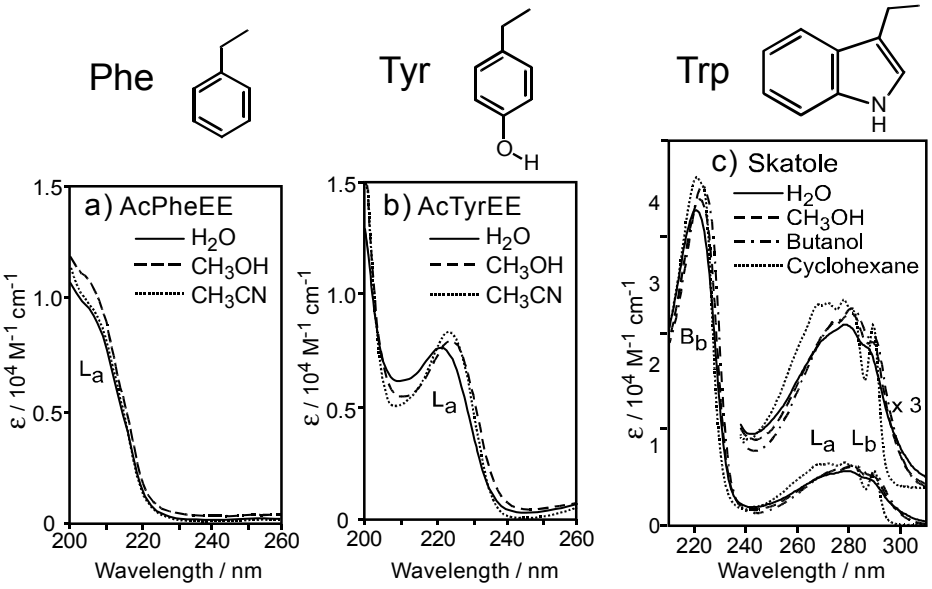

Fig. 9 UV absorption spectra of model compounds of Phe, Tyr, and Trp dissolved in various solvents.[33,34] a) AcPheEE in H_2O, CH_3OH, and CH_3CN. b) AcTyrEE in H_2O, CH_3OH, and CH_3CN. c) Skatole in H_2O, CH_3OH, butanol, and cyclohexane.

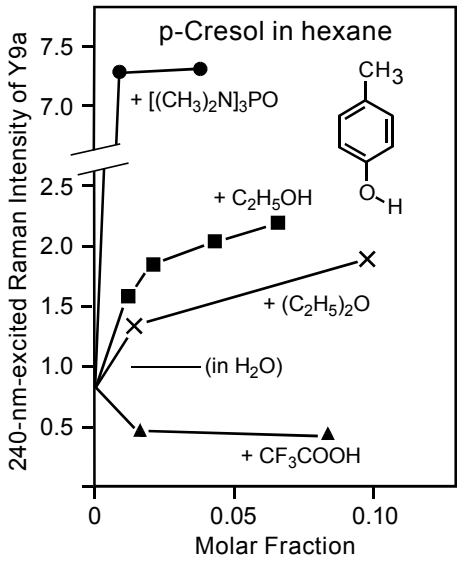

Fig. 10 Effects of hydrogen bonding on the 240-nm-excited Raman intensity of the Y9a band of *p*-cresol dissolved in hexane.[40] Small amounts of hexamethylphosphoramide, ethanol, diethyl ether, or trifluoroacetic acid were added to the hexane solution. The abscissa represents the mole fraction of the added hydrogen bonding acceptor or donor. The intensity is indicated as a relative value to that in H_2O (horizontal bar).

observations indicate that the UV Raman intensities of L_a-resonant bands of Phe are a very sensitive marker of environmental polarity.

The phenol ring of Tyr and the indole ring of Trp can form hydrogen bonds, and the UV absorption bands of these aromatic rings are affected not only by the environmental polarity but also by hydrogen bonding. Among hydrogen bonding solvents, CH_3OH is less polar than H_2O.[35,36] Accordingly, the solvent change from H_2O to CH_3OH may be used to monitor the effect of polarity decrease without affecting the hydrogen bonding state. The UV absorption spectra in Fig. 9b show that the L_a absorption of the Tyr phenol ring is stronger in CH_3OH than in H_2O, suggesting that the Raman intensity increases with decrease of environmental polarity. Analogous solvent effects are also seen for the B_b and L_a absorption bands of the Trp indole ring (Fig. 9c). Comparison of the Raman spectra excited at 229 nm and longer wavelengths has shown that the side chains of Tyr and Trp give stronger Raman bands in less polar environments provided that the hydrogen bonding state is unaltered.[33,34,39]

The UV absorption of the His imidazole ring is much weaker than those of Phe, Tyr, and Trp (Fig. 2), and no solvent effects have been reported on the Raman intensity of His. The imidazole ring has two nitrogen atoms that can be involved in hydrogen bonding. Effects of environmental polarity on Raman bands of His, if any, may be smaller than hydrogen bonding effects.

3·5 Hydrogen bonding

Hydrogen bonding affects molecular vibrations as well as electronic transitions. Therefore, the effect of hydrogen bonding is expected to appear both in the intensity and in the wavenumber of Raman bands. A small red-shift of the L_a absorption occurs for AcTyrEE upon solvent change from CH_3CN to CH_3OH (Fig. 9b). The red-shift suggests that hydrogen bonding enhances the Raman bands resonant with the L_a transition when excited at a wavelength longer than the peak wavelength (λ_{max}) of the L_a band. Figure 10 demonstrates a dramatic effect of hydrogen bonding on the 240-nm-excited Raman intensity of the Tyr Y9a band at 1180 cm^{-1}.[40] In this experiment, *p*-cresol, a model compound of Tyr, was first diluted in non-hydrogen-bonding hexane and then a trace amount of a third component was added. When the third component was a stronger proton acceptor than *p*-cresol, the Y9a Raman intensity increased two or more times depending on the strength of the proton acceptor ($[(CH_3)_2N]_3PO$, C_2H_5OH, and $(C_2H_5)_2O$ in Fig. 10). On the contrary, when the third component was a stronger proton donor than *p*-cresol, the Y9a intensity decreased to about a half (CF_3COOH in Fig. 10). These observations clearly indicate that the UV Raman intensity of the Tyr Y9a band can be used as a marker of hydrogen bonding. The intensity of the Y9a Raman band is high when the phenolic OH group of Tyr acts as a proton donor, while it is low when the OH group is involved in hydrogen bonding as a proton acceptor. In the donor-acceptor or non-hydrogen bonding state, the intensity is medium. Taken together with the effect of environmental polarity described in the preceding section, the L_a-resonant Raman bands are expected to be strongest when the phenol ring is hydrogen bonded as a proton donor in non-polar environments.

In contrast to the phenol ring of Tyr, the indole ring of Trp can act only as a proton donor in hydrogen bonding. As was observed for the Tyr L_a band, a red-shift occurs for the B_b absorption band of skatole on going from non-hydrogen-bonding cyclohexane solution to hydrogen-bonding CH_3OH and butanol solutions (Fig. 9c). The Raman bands resonant with the B_b transition are thus expected to be enhanced when excited at a wavelength longer than the λ_{max} of the B_b band. Actually, enhancement of Raman bands in the proton donor state has been observed for the B_b-resonant Raman bands (W3, W7, W16, and W18) with 229 nm and longer wavelength excitation.[34] Similarly to the case of L_a-resonant Raman bands of Tyr, the B_b-resonant Raman bands of Trp are expected to be strongest when the indole ring is hydrogen bonded as a proton donor in non-polar environments.[34]

Hydrogen bonding also affects the wavenumbers of Raman bands of Tyr, Trp, and His. Although the O–H or N–H stretching mode of the aromatic ring is expected to be most sensitive to hydrogen bonding, the Raman bands of such vibrations of Tyr, Trp, and His are not resonance enhanced even with UV excitation and are covered by the O–H stretching band of solvent H_2O. Accordingly, one must find other vibrations that are sensitive to hydrogen bonding and enhanced with UV excitation.

The Tyr Y7a′ band around 1260 cm^{-1} (Fig. 3b) arises from the C–O stretching vibration of the phenol ring. This vibrational mode makes the Y7a′ band sensitive to the state of hydrogen bonding at the phenolic OH site. The Y7a′ band appears around 1265, 1240, and 1255 cm^{-1} when the OH group acts as a proton donor, acceptor, and donor/acceptor, respectively.[41] On the other hand, the Y8a band around 1615 cm^{-1} and the Y8b band around 1600 cm^{-1} (Fig. 3b) are reported to shift to lower wavenumbers with increase of the proton donation to an acceptor.[38,42]

Another hydrogen bonding marker of Tyr is the doublet at 850/830 cm^{-1} (Fig. 3b), which arises from a Fermi resonance (vibrational coupling) between the fundamental of the Y1 in-plane vibration and the first overtone of an out-of-plane vibration of the phenol ring. Hydrogen bonding is considered to affect the Fermi resonance through alternation of the relative wavenumber positions of the fundamental and overtone bands, resulting in a change of the doublet intensity ratio (I_{850}/I_{830}).

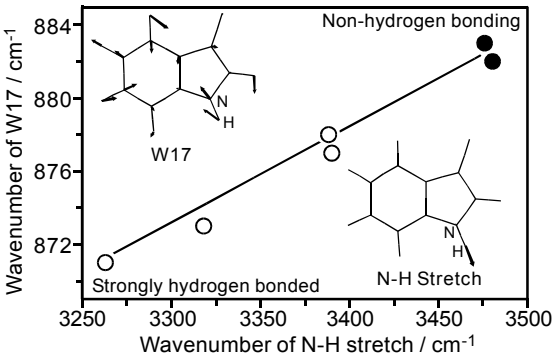

Fig. 11 Plot of the wavenumber of the W17 band against that of the indole N–H stretching vibration observed for Trp model compounds in crystals (open circle) or in solution (filled circle).[43] The N–H stretch wavenumbers were measured by infrared absorption spectroscopy. The insets show the vibrational modes of W17 and the N–H stretch.

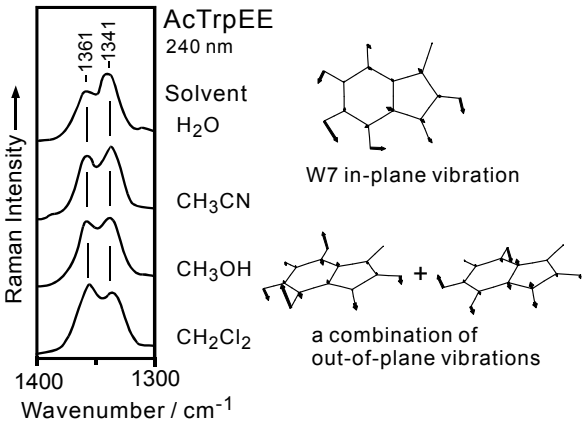

Fig. 12 Solvent effect on the W7 doublet of Trp in 240-nm-excited Raman spectra. *N*-Acetyl-L-tryptophan ethyl ester (AcTrpEE) was dissolved in H_2O, CH_3CN, CH_3OH, and CH_2Cl_2. The right half of the figure shows the vibrational mode of W7 and those of two out-of-plane vibrations, whose combination is likely to be in Fermi resonance with W7.

With visible light excitation, the I_{850}/I_{830} value was found to be about 0.3, 2.5, and 1.25 when the phenolic OH group acts as a proton donor, acceptor, and donor/acceptor, respectively.[43] The doublet was reported to become a singlet when the phenol ring is not hydrogen bonded in a strongly hydrophobic environment or *in vacuo*.[44,45] This observation raises the possibility that the Fermi resonance may also be affected by intermolecular interactions other than hydrogen bonding. In UV Raman spectra, the intensity ratio I_{850}/I_{830} slightly deviates from the values found with visible light excitation. For example, amino acid Tyr dissolved in H_2O, which is expected to be in the donor/acceptor state and to give a I_{850}/I_{830} ratio of about 1.25, actually exhibits a ratio of 1.7 in the 244-nm-excited Raman spectrum (Fig. 3b).

The wavenumber of the W17 band of Trp around 880 cm^{-1} (Fig. 3c) is known to be sensitive to hydrogen bonding.[46] Figure 11 shows a plot of the W17 wavenumber against the wavenumber of the indole N–H stretch vibration observed for model compounds in the crystalline state or in solution. (The N–H stretch vibration was monitored by infrared absorption spectroscopy.) Since the wavenumber of the N–H stretch vibration decreases with increase of the strength of hydrogen bonding, the positive correlation between the two wavenumbers in Fig. 11 indicates that the W17 wavenumber also decreases with increase of the strength of hydrogen bonding. The W17 wavenumber is lowest at ~871 cm^{-1} in the strongly hydrogen-bonded state and highest at ~883 cm^{-1} in the non-hydrogen-bonding state. The W17 band can be identified in UV resonance Raman spectra of proteins and serves as a marker of hydrogen bonding at the indole N–H site of Trp.

As described in Sect. 3·2, the $\nu(C_4{=}C_5)$ and $\nu(N_\tau C_2 N_\pi)$ wavenumbers of *N*-deuterated imidazolium, $HisD^+$, are sensitive to hydrogen bonding. Although some vibrations of the neutral form of His might also be sensitive to hydrogen bonding, the Raman intensity in the neutral form is weak and no Raman spectral data are available about the hydrogen bonding effect on neutral His.

3·6 Hydrophobic interaction

In aqueous solution, non-polar molecules cluster together and exclude water molecules from the clustering region to minimize the disturbance to the hydrogen-bonding network of water. Such clustering of non-polar molecules in water is called the hydrophobic effect, though the main contributor to the stability of the hydrophobic cluster comes from the free energy of the surrounding water system.[47,48] Within the hydrophobic cluster, non-polar molecules are attracting each other by van der Waals forces, and such hydrophobic interaction affects the force field for molecular vibrations, resulting in changes of vibrational wavenumbers.

An example of the effect of hydrophobic interaction on the vibrational wavenumber is seen for Trp. The W7 in-plane vibration of Trp gives a doublet around 1360/1340 cm^{-1} in Raman spectra (Fig. 3c) and the appearance of the doublet is ascribed to a Fermi resonance between the W7 fundamental vibration and a combination of out-of-plane vibrations.[49] From visible-light-excited Raman spectra of model compounds dissolved in various solvents, the doublet intensity ratio I_{1360}/I_{1340} was shown to increase with increase of the hydrophobic interaction. Figure 12 shows the 240-nm-excited Raman spectra of *N*-acetyl-L-tryptophan ethyl ester (AcTrpEE) dissolved in H_2O, CH_3CN, CH_3OH, and CH_2Cl_2. The hydrophobic interaction between the solute and solvent is expected to increase with the solvent hydrophobicity. Actually, with increase of the solvent hydrophobicity,[50] the W7 intensity ratio I_{1360}/I_{1340} increases from about 0.7 to 1.2, as seen in Fig. 12. The dependence of I_{1360}/I_{1340} on the hydrophobic interaction may be accounted for by a change in the relative wavenumber positions of the fundamental and combination bands caused by van der Waals forces. The doublet has been found to become a triplet when the hydrophobic interaction is unusually strong,[51] suggesting an involvement of another combination in the Fermi resonance with W7.

With excitation at a wavelength of ≤230 nm, the value of I_{1360}/I_{1340} is significantly increased compared to that observed with excitation at ≥240 nm.[52,53] Probably, with excitation at ≤230 nm, the 1360 cm^{-1} component of the doublet is overlapped by a combination or overtone band that is not involved in the Fermi resonance with W7 but is enhanced through resonance with the B_b absorption at 218 nm (Fig. 2). The utility of the W7 doublet intensity ratio I_{1360}/I_{1340} as a marker of hydrophobic interaction may be limited only to cases when the Raman spectrum is excited at ≥240 nm. The I_{1360}/I_{1340} values observed with 230-nm excitation for model compounds dissolved in varied solvents were reported to show a dependence on the solvent polarity/polarizability.[53]

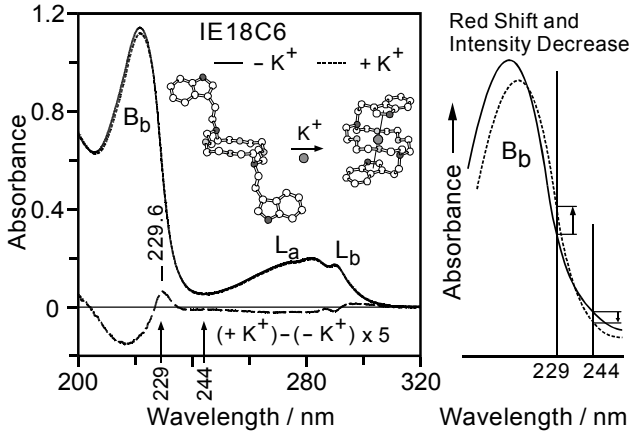

Fig. 13 Effect of cation-π interaction on the UV absorption spectrum of the indole ring.[27] The absorption spectra of *N*,*N*′-bis(2-(3-indolyl)-ethyl)-4,13-diaza-18-crown-6 (IE18C6) in the presence and absence of the K^+ ion are compared. The difference spectrum in the bottom trace indicates a small red-shift of the B_b absorption band accompanied by an intensity decrease upon the cation-π interaction. The change of the B_b absorption band is exaggeratedly illustrated in the right section.

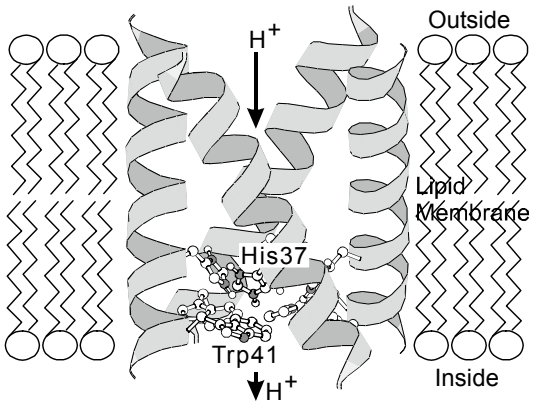

Fig. 14 Model for the M2 proton channel incorporated into lipid membranes.[27,28] A bundle of four identical transmembrane helices forms a proton-permeable channel. His37 and Trp51 are the key residues in the channel activity.

3·7 Cation-π interaction

The π-electron system of an aromatic ring attracts a positive charge in the neighborhood with an interaction energy comparable to that of a hydrogen bond.[54] The cation-π interaction is increasingly recognized as an important factor that takes part in protein structure and function. The aromatic rings of Phe, Tyr, and Trp can serve as a π-electron system in the interaction with the cationic side chains of Arg, Lys, and cationic His as well as with the amino terminus NH_3^+. Many cation-π interactions involving aromatic residues have been identified in protein crystal structures revealed by X-ray diffraction or in solution structures revealed by NMR on the basis of proximity between the π-electron system and the cation.[54,55]

Among the aromatic rings of amino acids, the indole ring of Trp is known to be best suited for the cation-π interaction.[54,55] Figure 13 shows the effect of cation-π interaction on the absorption spectrum of *N*,*N*′-bis(2-(3-indolyl)ethyl)-4,13-diaza-18-crown-6 (IE18C6), which contains two indole rings linked to the nitrogen atoms of diaza-18-crown-6. The crown ether ring of the model compound captures a K^+ ion and the indole side arms sandwich the captured cation.[56] Although the effect of K^+ binding on the absorption spectrum is not large, it is evident from the difference spectrum that the indole-K^+ interaction induces a small red-shift of the B_b absorption accompanied by an intensity decrease.[27] This type of change in absorption spectrum has not been observed in solvent effect studies (Fig. 9c). In the right section of Fig. 13, the unusual change of the B_b absorption is schematically depicted. The cation-π interaction causes an increase of the absorption intensity at 229 nm and a decrease at 244 nm, predicting an intensity increase and a decrease of B_b-resonant Raman bands excited at 229 and 244 nm, respectively. Actually, in the presence of cation-π interaction, the W1, W3, and W16 Raman bands of IE18C6 become stronger and weaker when excited at 229 and 244 nm, respectively.[27] The Trp indole ring has also been found to undergo a cation-π interaction with the Cu ion.[57,58] For Phe and Tyr, no Raman markers of cation-π interaction have been reported.

4 Application of Raman Markers

The Raman markers of structures and interactions described above have been applied to many proteins. Among the markers, those based on the wavenumber of a Raman band can be used not only in UV resonance Raman spectroscopy but also in non-resonance Raman spectroscopy with visible-light excitation. The usefulness of the Raman markers has been verified in studies on structures and functions of various kinds of proteins including enzymes, bioactive peptides, and membrane-bound proteins. An example of such applications will be briefly described below.

The M2 protein of influenza A virus forms a transmembrane homotetramer, which is activated as a proton channel at acidic pH and plays an important role in the virus infection. Each polypeptide chain of the M2 protein is composed of 97 amino acid residues with a putative transmembrane domain composed of about 25 residues including His at position 37 and Trp at position 41. To study the roles of His37 and Trp41 in the proton channel activity, we incorporated a peptide representing the M2 transmembrane domain (M2-TMP) into model lipid membranes (Fig. 14), and then we examined the structure of the channel by UV Raman spectroscopy.[27]

Figures 15a and 15b show 244-nm-excited Raman spectra of the M2-TMP channel suspended in D_2O at pD 7.4 and 5.4, respectively. The spectrum at pD 5.4 exhibits a weak Raman band at 1407 cm^{-1}, which is ascribed to $\nu(N_\tau C_2 N_\pi)$ of $HisD^+$ (a protonation marker, see Sect. 3·1). On the other hand, Raman bands assignable to Trp51 (W1, W3, W17, and W16) are weak at pD 5.4 compared to pD 7.4. The intensities of the $\nu(N_\tau C_2 N_\pi)$ and W1 bands are plotted against pD in Figs. 15e and 15f, respectively. The midpoint of intensity change is seen at pD 5.7 for both bands, indicating that the imidazole ring of His37 is protonated below pD 5.7 and that the cationic imidazole ring interacts with the indole ring of Trp51. Further examination of Raman spectra with 229-nm excitation shows that the protonation of His37 causes intensity increases of Trp Raman bands (Fig. 15d) unlike the decreases observed with 244-nm excitation (Fig. 15c). This type of intensity change is characteristic of cation-π interaction (see Sect. 3·7). Since the channel is activated below pH 5.8, the Raman spectroscopic findings strongly suggest that the protonation of His37 and the resultant cation-π interaction between His37 and Trp51 play a

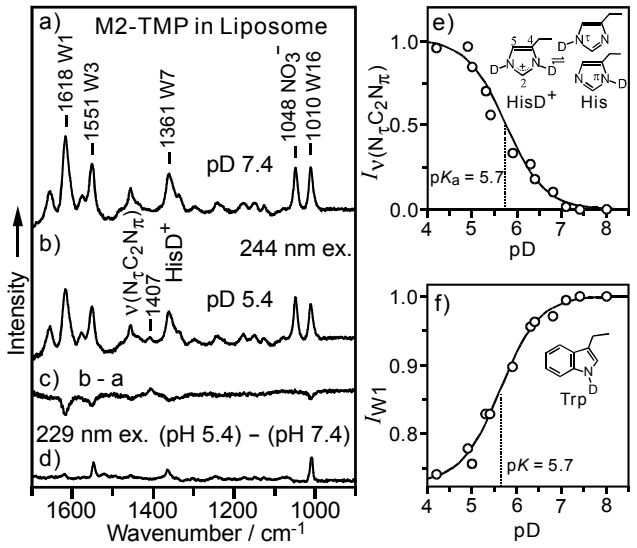

Fig. 15 244-nm-excited Raman spectra of M2-TMP incorporated into lipid membranes suspended in D_2O at a) pD 7.4 and b) pD 5.4.[27] c) Difference spectrum, spectrum b minus spectrum a. d) Difference spectrum between pH 5.4 and 7.4 measured with 229-nm excitation. e) 244-nm Raman intensity of the $\nu(N_\tau C_2 N_\pi)$ band of *N*-deuterated cationic His37 ($HisD^+$) plotted as a function of pD. f) 244-nm Raman intensity of the W1 band of Trp51 plotted against pD. The intensities in these plots were normalized relative to the maximum intensity.

role in the activation of the M2 proton channel.

Additionally, the W3 wavenumber was observed to change from 1553 to 1550 cm^{-1} upon activation of the channel, suggesting a small reorientation of the Trp41 indole ring (see Sect. 3·2). The W17 Raman band appeared at 878 cm^{-1} irrespective of pH, indicating that the indole ring of Trp41 is involved in a medium-strength hydrogen bond in both the active and the inactive states of the channel (see Sect. 3·5). The intensity ratio of the W7 doublet I_{1360}/I_{1340} was observed to be much greater than unity, suggesting a strong hydrophobic interaction of the Trp51 indole ring (see Sect. 3·6). On the basis of these Raman spectroscopic findings, a molecular model for the M2 channel activation was proposed.[27,28] UV Raman spectroscopy has also been utilized to build a model for the proton channel of influenza B virus.[59]

5 Concluding Remarks

Raman bands of aromatic ring vibrations are selectively enhanced with UV excitation, and therefore UV Raman spectroscopy serves as a powerful tool for investigating the structures and interactions of the aromatic side chains of Phe, Tyr, Trp, and His in proteins. Intensities and wavenumbers of UV Raman bands arising from aromatic side chains are affected by many structural factors and interactions, such as protonation/deprotonation, conformation, metal coordination, environmental polarity, hydrogen bonding, hydrophobic interaction, and cation-π interaction. To extract structural information from the observed Raman spectra, Raman markers based on empirical spectra-structure correlations are useful, as reviewed in this article. Although many Raman markers have so far been discovered, new markers, giving not only qualitative but also quantitative pictures, are still demanded. Future advances in experimental technology for obtaining high-quality UV Raman spectra and in theoretical analysis of spectra-structure correlations will make UV Raman spectroscopy more powerful in the structural analysis of aromatic residues, which sometimes play critical roles in protein functions.

6 References

1. D. A. Long, "*Raman Spectroscopy*", **1977**, McGraw-Hill, New York.
2. J. Tang and A. C. Albrecht, "*Raman Spectroscopy: Theory and Practice*", ed. H. A. Szymanski, **1970**, Vol. 2, Chap. 2, Plenum Press, New York, 33.
3. M. D. Morris and D. J. Wallan, *Anal. Chem.*, **1979**, *51*, 182A.
4. R. P. Rava and T. G. Spiro, *J. Am. Chem. Soc.*, **1984**, *106*, 4062.
5. R. P. Rava and T. G. Spiro, *J. Phys. Chem.*, **1985**, *89*, 1856.
6. I. Harada and H. Takeuchi, "*Spectroscopy of Biological Systems*", ed. R. J. H. Clark and R. E. Hester, **1986**, Chap. 3, John Wiley & Sons, Chichester, 113.
7. S. A. Asher, M. Ludwig, and C. R. Johnson, *J. Am. Chem. Soc.*, **1986**, *108*, 3186.
8. M. Ludwig and S. A. Asher, *J. Am. Chem. Soc.*, **1988**, *110*, 1005.
9. S. P. A. Fodor, R. A. Copeland, C. A. Grygon, and T. G. Spiro, *J. Am. Chem. Soc.*, **1989**, *111*, 5509.
10. S. Hashimoto, T. Ikeda, H. Takeuchi, and I. Harada, *Appl. Spectrosc.*, **1993**, *47*, 1283.
11. G. R. Grimsley, J. M. Scholtz, and C. N. Pace, *Protein Sci.*, **2009**, *18*, 247.
12. I. Ashikawa and K. Itoh, *Biopolymers*, **1979**, *18*, 1859.
13. K. Hasegawa, T. Ono, and T. Noguchi, *J. Phys. Chem. B*, **2000**, *104*, 4253.
14. A. Toyama, K. Ono, S. Hashimoto, and H. Takeuchi, *J. Chem. Phys. A*, **2002**, *106*, 3403.
15. A. Toyama, Y. Takahashi, and H. Takeuchi, *Biochemistry*, **2004**, *43*, 4670.
16. M. Tasumi, I. Harada, T. Takamatsu, and S. Takahashi, *J. Raman Spectrosc.*, **1982**, *12*, 149.
17. R. C. Lord and N.-T. Yu, *J. Mol. Biol.*, **1970**, *51*, 203.
18. H. Takeuchi, I. Harada, and H. Yoshida, *Biochim. Biophys. Acta*, **1991**, *1078*, 307.
19. S. Hashimoto and H. Takeuchi, *J. Am. Chem. Soc.*, **1998**, *120*, 11012.
20. Q. Wu, F. Li, W. Wang, M. H. Hecht, and T. G. Spiro, *J. Inorg. Biochem.*, **2002**, *88*, 381.
21. S. Hashimoto and H. Takeuchi, *Biochemistry*, **2006**, *45*, 9660.
22. H. Takeuchi and I. Harada, *Spectrochim. Acta*, **1986**, *42A*, 1069.
23. T. Miura, H. Takeuchi, and I. Harada, *J. Raman Spectrosc.*, **1989**, *20*, 667.
24. T. Maruyama and H. Takeuchi, *J. Raman Spectrosc.*, **1995**, *26*, 319.
25. M. J. McGregor, S. A. Islam, and M. J. E. Sternberg, *J. Mol. Biol.*, **1987**, *198*, 295.
26. T. Maruyama and H. Takeuchi, *Biochemistry*, **1997**, *36*, 10993.
27. A. Okada, T. Miura, and H. Takeuchi, *Biochemistry*, **2001**, *40*, 6053.
28. H. Takeuchi, A. Okada, and T. Miura, *FEBS Lett.*, **2003**, *552*, 35.
29. H. Takeuchi, Y. Kimura, I. Koitabashi, and I. Harada, *J. Raman Spectrosc.*, **1991**, *22*, 233.

30. H. Hiramatsu, N. Miki, and H. Takeuchi, *J. Raman Spectrosc*., **2010**, *41*, 1708.
31. H. Takeuchi, *Biopolymers*, **2003**, *72*, 305.
32. T. Miura, T. Satoh, A. Hori-i, and H. Takeuchi, *J. Raman Spectrosc*., **1998**, *29*, 41.
33. H. Takeuchi, Y. Ohtsuka, and I. Harada, *J. Am. Chem. Soc*., **1992**, *114*, 5321.
34. M. Matsuno and H. Takeuchi, *Bull. Chem. Soc. Jpn*., **1998**, *71*, 851.
35. Y. Marcus, *Chem. Soc. Rev*., **1993**, *22*, 409.
36. A. R. Katritzky, D. C. Fara, H. Yang, and K. Tämm, *Chem. Rev*., **2004**, *104*, 175.
37. C. Su, Y. Wang, and T. G. Spiro, *J. Raman Spectrosc*., **1990**, *21*, 435.
38. P. G. Hildebrandt, R. A. Copeland, and T. G. Spiro, *Biochemistry*, **1988**, *27*, 5426.
39. N. Cho and S. A. Asher, *Biospectroscopy*, **1996**, *2*, 71.
40. S. Hashimoto, T. Yabusaki, H. Takeuchi, and I. Harada, *Biospectroscopy*, **1995**, *1*, 375.
41. H. Takeuchi, N. Watanabe, Y. Satoh, and I. Harada, *J. Raman Spectrosc*., **1989**, *20*, 233.
42. K. R. Rodgers, C. Su, S. Subramaniam, and T. G. Spiro, *J. Am. Chem. Soc*., **1992**, *114*, 3697.
43. M. N. Siamwiza, R. C. Lord, M. C. Chen, T. Takamatsu, I. Harada, H. Matsuura, and T. Shimanouchi, *Biochemistry*, **1975**, *14*, 4870.
44. S. A. Overman, K. L. Aubrey, N. S. Vispo, G. Cesareni, and G. J. Thomas, Jr., *Biochemistry*, **1994**, *33*, 1037.
45. Z. Arp, D. Autrey, J. Laane, S. A. Overman, and G. J. Thomas, Jr., *Biochemistry*, **2001**, *40*, 2522.
46. T. Miura, H. Takeuchi, and I. Harada, *Biochemistry*, **1988**, *27*, 88.
47. T. Lazaridis, *Acc. Chem. Res*., **2001**, *34*, 931.
48. D. Chandler, *Nature*, **2005**, *437*, 640.
49. I. Harada, T. Miura, and H. Takeuchi, *Spetcrochim. Acta*, **1986**, *42A*, 307.
50. Y. Marcus, "*The Properties of Solvents*", **1998**, John Wiley & Sons, Chichester, 175.
51. S. Hashimoto, K. Obata, H. Takeuchi, R. Needleman, and J. K. Lanyi, *Biochemistry*, **1997**, *36*, 11583.
52. I. R. Rodriguez-Mendieta, G. R. Spence, C. Gell, S. E. Radford, and D. A. Smith, *Biochemistry*, **2005**, *44*, 11583.
53. D. E. Schlamadinger, J. E. Gable, and J. E. Kim, *J. Phys. Chem. B*, **2009**, *113*, 14769.
54. J. C. Ma and D. A. Dougherty, *Chem. Rev*., **1997**, *97*, 1303.
55. J. P. Gallivan and D. A. Dougherty, *Proc. Natl. Acad. Sci. U. S. A*., **1999**, *96*, 10566.
56. S. L. De Wall, E. S. Meadows, L. J. Barbour, and G. W. Gokel, *J. Am. Chem. Soc*., **1999**, *121*, 5613.
57. Y. Xue, A. V. Davis, G. Balakrishnan, J. P. Stasser, B. M. Staehlin, P. Focia, T. G. Spiro, J. E. Penner-Hahn, and T. V. O'Halloran, *Nat. Chem. Biol*., **2008**, *4*, 107.
58. H. Yorita, K. Otomo, H. Hiramatsu, A. Toyama, T. Miura, and H. Takeuchi, *J. Am. Chem. Soc*., **2008**, *130*, 15266.
59. K. Otomo, A. Toyama, T. Miura, and H. Takeuchi, *J. Biochem*., **2009**, *145*, 543.